



OPEN ACCESS

EDITED BY

Vittorio Palmieri,
Azienda Ospedaliera dei Colli, Italy

REVIEWED BY

Md Habibur Rahman,
Rutgers, The State University
of New Jersey, United States
Andreas von Knethen,
Goethe University Frankfurt, Germany

*CORRESPONDENCE

Saiqi Li
lisaiqi@ashchest.org
Bin He
bin_he@sjtu.edu.cn

†These authors have contributed
equally to this work

SPECIALTY SECTION

This article was submitted to
General Cardiovascular Medicine,
a section of the journal
Frontiers in Cardiovascular Medicine

RECEIVED 02 August 2022

ACCEPTED 20 October 2022

PUBLISHED 07 November 2022

CITATION

Liu W, Guo X, Jin L, Hong T, Zhang Q,
Su F, Shen Y, Li S and He B (2022)
Lipocalin-2 participates
in sepsis-induced myocardial injury
by mediating lipid accumulation
and mitochondrial dysfunction.
Front. Cardiovasc. Med. 9:1009726.
doi: 10.3389/fcvm.2022.1009726

COPYRIGHT

© 2022 Liu, Guo, Jin, Hong, Zhang, Su,
Shen, Li and He. This is an
open-access article distributed under
the terms of the [Creative Commons
Attribution License \(CC BY\)](https://creativecommons.org/licenses/by/4.0/). The use,
distribution or reproduction in other
forums is permitted, provided the
original author(s) and the copyright
owner(s) are credited and that the
original publication in this journal is
cited, in accordance with accepted
academic practice. No use, distribution
or reproduction is permitted which
does not comply with these terms.

Lipocalin-2 participates in sepsis-induced myocardial injury by mediating lipid accumulation and mitochondrial dysfunction

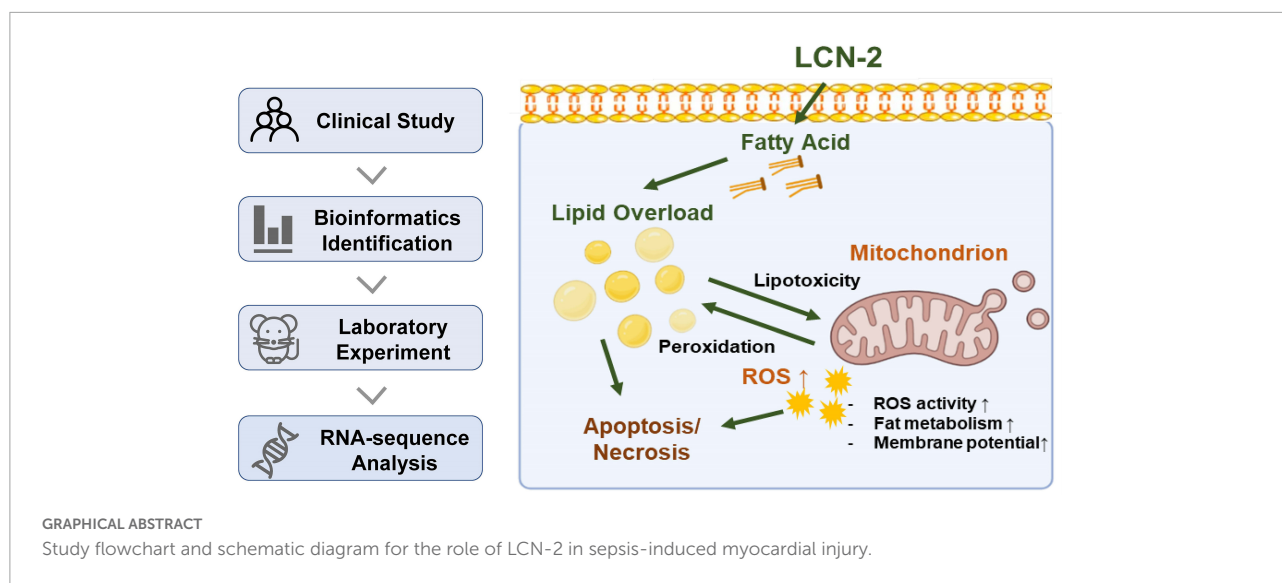
Weizhuo Liu^{1,2†}, Xiaoyu Guo^{1,2†}, Lei Jin^{1†}, Ting Hong^{1,2},
Qianyun Zhang¹, Fan Su¹, Yi Shen¹, Saiqi Li^{1*} and Bin He^{1*}

¹Department of Critical Care Medicine, Shanghai Chest Hospital, Shanghai Jiao Tong University School of Medicine, Shanghai, China, ²Center for Cardiopulmonary Translational Medicine, Shanghai Chest Hospital, Shanghai Jiao Tong University School of Medicine, Shanghai, China

Background: Sepsis-induced cardiomyopathy (*SIC*) is one major cause of death for sepsis but lacks timely diagnosis and specific treatment due to unclear mechanisms. Lipocalin-2 (*LCN-2*) is a key regulator of lipid metabolism which has been recently proved closely related to sepsis, however, the relationship between *LCN-2* and septic myocardial injury remains unknown. We aim to explore the role of *LCN-2* in the pathological progress of *SIC* based on clinical and laboratory evidence.

Methods: Consecutive patients admitted to the intensive care unit (ICU) from August 2021 to April 2022 fulfilling the criteria of severe sepsis were included. The level of *LCN-2* in plasma was assayed and analyzed with clinical characteristics. Biostatistical analysis was performed for further identification and pathway enrichment. Mouse model for *SIC* was thereafter established, in which plasma and tissue *LCN-2* levels were tested. RNA sequencing was used for verification and to reveal the possible mechanism. Mitochondrial function and intracellular lipid levels were assayed to further assess the biological effects of targeting *LCN-2* in cardiomyocytes with small interference RNAs (siRNAs).

Results: The level of *LCN-2* in plasma was markedly higher in patients with severe sepsis and was associated with higher cardiac biomarkers and lower LVEF. In the *in vivo* experiment, circulating *LCN-2* from plasma was found to increase in *SIC* mice. A higher level of *LCN-2* transcription in myocardial tissue was also found in *SIC* and showed a clear time relationship. RNA sequencing analysis showed the level of *LCN-2* was associated with several gene-sets relevant to mitochondrial function and lipid metabolism-associated pathways. The suppression of *LCN-2* protected mitochondrial morphology and limited the production of ROS, as well as restored the mitochondrial membrane potential damaged by LPS. Neutral lipid staining showed prominent lipid accumulation in LPS group, which was alleviated by the treatment of si*LCN2*.



Conclusion: The level of LCN-2 is significantly increased in *SIC* at both circulating and tissue levels, which is correlated with the severity of myocardial injury indicators, and may work as an early and great predictor of *SIC*. LCN-2 probably participates in the process of septic myocardial injury through mediating lipid accumulation and affecting mitochondrial function.

KEYWORDS

lipocalin-2, sepsis, myocardial injury, lipid metabolism, mitochondrial dysfunction

Introduction

Sepsis is the life-threatening organ dysfunction caused by a dysregulated host response to infection (1, 2). Cardiac dysfunction or injury caused by sepsis, i.e., sepsis-induced cardiomyopathy (*SIC*), manifesting clinically as decreased myocardial contractility, weakened response to cardiac preload, etc., is one of the leading causes of death for sepsis (3, 4). However, timely diagnosis and potential therapeutic targets still remain a major challenge in the management of *SIC*, in which discovering novel biomarkers can be helpful (4).

Lipid metabolism is vital for maintaining the normal function of mitochondria which plays an important role in *SIC* (5, 6). The disorder of lipid metabolism increases reactive oxygen species (ROS) production and fission of mitochondrial, leading to mitochondrial dysfunction and cell apoptosis (7–9). Recent studies have revealed the disorder of lipid metabolism in several kinds of sepsis-induced organ injury (10, 11), which has also been observed in septic myocardial tissue in our previous work (12), however, *via* unclear mechanisms.

Lipocalin-2 (LCN-2), also known as neutrophil gelatinase-associated lipocalin (NGAL), is an innate immune protein mainly responsible for the transportation of lipids, iron, etc., acting as an upstream regulator of lipid metabolism (13). It has broad expression in various tissues and cell types including cardiomyocytes and endothelial cells, which has been recognized as an emerging player in different physiological and pathological processes, including iron homeostasis, mitochondria function, inflammation, microbial infection, etc. (14, 15).

It has been found that LCN-2 participates in the development of heart failure, myocardial hypertrophy, myocardial ischemia-reperfusion injury, chemotherapy-related cardiac function injury, and other heart diseases (16–18). Recent studies have also shown its close correlation to the severity of sepsis (19, 20), the relationship between LCN-2 and septic myocardial injury, however, remains unclear. In this study, we aim to explore the role of LCN-2 in the pathological progress of septic myocardial injury based on clinical and laboratory evidence, as well as its potential mechanism.

Materials and methods

Materials and reagents

Materials and reagents were included in [Supplementary material](#).

Clinical study population and data collection

Patients admitted to the intensive care unit (ICU) from August 2021 to April 2022 who fulfilled the criteria for severe sepsis or septic shock (1) and were 18 years or older were consecutively included. Patients with previous myocardial infarction, heart failure with reduced ejection fraction, moderate to severe valve diseases and phase 4/5 chronic kidney disease, or those with a history of percutaneous coronary angioplasty or coronary bypass surgery, or those without risk evaluation or proper resuscitation therapy in accordance with the guide for sepsis bundle, were excluded from the study. Those with missing data pertaining to sex, date of birth, diagnosis or lack of important examination data were also ruled out. A control group was set up with individuals without any evidence of sepsis and free of any heart diseases at baseline. The study was approved by the Institutional Review Board (IRB) for Human Research at Shanghai Chest Hospital Shanghai Jiao Tong University in August 2021 entitled Early Diagnosis and Prognostic Assessment in Sepsis-Induced Myocardial Injury (approval No. KS(Y)22061), and conducted in accordance with the ethical standards of the IRB on human research and with the Helsinki Declaration of 1975. Informed consent was obtained from patients at the time of enrollment.

The clinical history of all patients including age, gender, comorbidities, and laboratory results were retrieved from the hospital information system. In both groups, plasma was centrifuged within 30 min and plasma was stored at -80°C for subsequent analysis. Plasma LCN-2 was determined using Human Lipocalin ELISA Kit (RayBiotech, United States). Plasma chemistry, myocardial enzyme and markers, arterial blood gas analyses, and other laboratory tests including C-reactive protein (CRP), procalcitonin (PCT), etc. were assayed at the same time by routine laboratory methods. All subjects had continuous electrocardiogram (ECG) monitoring and arterial cannulation for invasive pressure monitoring as part of standard clinical practice. The results of echocardiographic tests performed within 3 days were also acquired.

Bioinformatic identification based on gene expression omnibus database

Biostatistical analysis of transcriptome array datasets was used to further identify critical genes and enrich related

signaling pathways. Two microarray profile datasets GSE28750 and GSE57065 of raw gene expression downloaded from gene expression omnibus (GEO) datasets and processed *via* GEO2R¹ (21), were investigated to screen key genes in sepsis. Differential expression genes (DEGs) were identified by calculating fold changes and *P*-values between sepsis and control groups. In this study, the cut-off criteria are *P*-value < 0.01 and $|\log \text{fold change (FC)}| > 2$. Subsequently, the overlapping DEGs consisting of common up-regulated and common down up regulated were presented through Venn diagrams.

Gene Ontology (GO) (22) analysis and Kyoto Encyclopedia of Gene and Genomes (KEGG) (23) pathway enrichment analyses were applied to study DEGs at the function level. GO annotations include three items: molecular functions (MF), biological processes (BP), and cellular components (CC), and KEGG is a set of genes and protein pathways with close interaction relationships. In this study, an online visualized tool² was used for GO and pathway enrichment. STRING database was applied to build a protein-protein interaction (PPI) network for discovering hub genes. *P* < 0.05 was set as the cut-off criterion.

Model establishment

The cellular model of SIC was established by lipopolysaccharide (LPS, Sigma-Aldrich, United States)

- 1 <http://www.ncbi.nlm.nih.gov/geo/geo2r>
- 2 <https://www.omicshare.com/tools/>

TABLE 1 Baseline characteristics of the patients.

Variable	Severe sepsis/Sepsis shock	Control group	<i>P</i> -value
Age (years)	70.6 \pm 7.5	65.8 \pm 5.8	0.06
Male gender (n,%)	14 (93.3)	13 (86.7)	0.54
Hypertension (n,%)	6 (40.0)	4 (26.7)	0.44
Diabetes (n,%)	3 (20.0)	2 (13.3)	0.62
WBC ($\times 10^9$)	20.00 \pm 5.97	11.09 \pm 2.96	< 0.001
Neutrophil % (%)	92.78 \pm 0.03	84.11 \pm 0.07	< 0.001
C-reactive protein (mg/l)	236.64 \pm 66.49	89.96 \pm 74.66	< 0.001
Procalcitonin ($\mu\text{g/L}$)	2.73 [2.12, 4.61]	0.19 [0.12, 0.31]	< 0.001
LCN-2 (ng/ml)	87.81 [64.55, 209.16]	43.16 [32.56, 94.36]	0.015*
Pro-BNP (pg/ml)	3060 [2180, 4800]	368 [295, 527]	0.025
Serum creatine ($\mu\text{mol/l}$)	89.1 [67.9, 285.0]	65.3 [58.0, 78.0]	0.019
Bilirubin ($\mu\text{mol/L}$)	35.3 [16.3, 76.3]	19.1 [11.9, 25.08]	0.040
Mechanical ventilation (%)	12 (80.0)	4 (26.7)	0.003
Renal replacement therapy (%)	4 (26.7)	1 (6.7)	0.032

Clinical variables were expressed as a percentage (%) for categorical variables, mean with SD for normally distributed continuous variables, and median with IQR for discontinuous variables. LCN-2, Lipocalin-2; Pro-BNP, pro-type-B natriuretic peptide. **P* < 0.05 .

incubation based on reported protocol (12, 24). Briefly, H9C2 cells were cultured in DMEM containing 10 $\mu\text{g/ml}$ LPS for 12 h. Morphology of cardiomyocytes was observed. C57BL/6 mice weighing 25–28 g (GemPharmatech Co., China) were raised in a specific pathogen-free (SPF) environment. LPS was injected intraperitoneally (i.p.) at a dosage of 20 mg/kg for 12 h to induce cardiac injury. Cardiac markers were tested to validate the establishment of models. All experimental procedures and animal studies were approved by the Animal Ethics Committee of Shanghai Chest Hospital.

Assay of plasma lipocalin-2 level in mice model

Plasma was centrifuged for 30 min and plasma was stored at -80°C for subsequent analysis. Plasma LCN-2 was determined at 12 h from the onset of SIC using Mouse Lipocalin ELISA Kit (RayBiotech, United States) by ELISA test. Mean values were calculated and used for statistical analyses.

Quantitative polymerase chain reaction of myocardial tissue

The gene expression of myocardial tissue was determined by RT-quantitative polymerase chain reaction (qPCR) with SYBR Green. Relative expression was quantified to Rplp0 as the internal standard control. All primer sequences are listed in [Supplementary Table 1](#).

RNA sequencing and analysis

RNA was extracted from heart tissues of SIC mice at 12 h after LPS stimulation that was grown under the appropriate

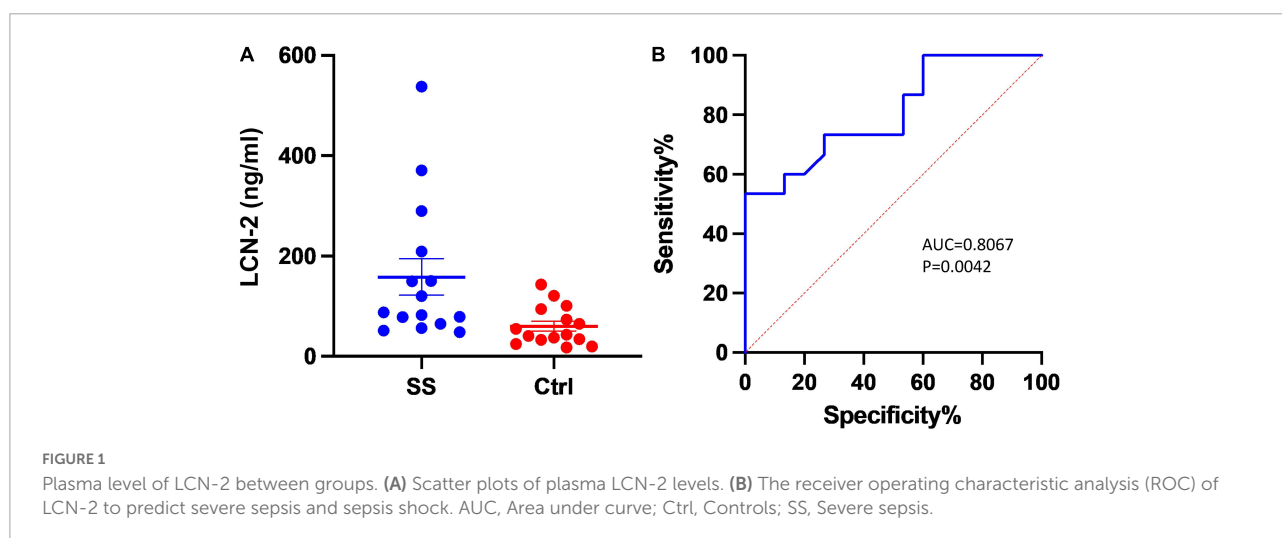
conditions using the RNeasy mini kit (Qiagen, United States). After that, RNA sequencing (RNA-seq) was performed by GENEWIZ (Suzhou, China). Genes with a | fold-change (FC) | > 2 and $P < 0.05$ were defined as significant differential expressed genes for further analysis. Gene Set Enrichment Analysis (GSEA) is a useful tool for the correlation analysis of different gene sets. We also used GSEA for function enrichment grouped by the high or low level (using the cut-off value calculated by Receiver Operator Characteristic curve) of LCN-2 in the RNA-sequence analysis.

Staining of cardiomyocyte

The intracellular lipid of H9C2 cells was detected and analyzed at 12 h after LPS induction using HCS LipidTOXTM (Invitrogen, United States). Laser scanning confocal microscope technology was then performed. The mitochondrial morphology and ROS level were assessed by MitoTrackerTM Red CMXRos (Invitrogen, United States) and DCFH-DA assessment (Invitrogen, United States) at 12 h after LPS stimulation, as well as the estimation of the mitochondrial membrane potential using the JC-1 probe (Invitrogen, United States).

Statistical analysis

Clinical variables were expressed as a percentage (%) for categorical variables, mean with standard deviation (SD) for normally distributed continuous variables, and median with interquartile rate (IQR) for discontinuous variables. To compare categorical variables, chi-square test or Fisher's exact test was used; to compare continuous variables, an unpaired two-tailed *t*-test or Mann–Whitney *U*-test was used. Patients with severe sepsis were then divided into low/high LCN-2 subgroups



according to the 75th percentile following classic classification method (25, 26) in the following subgroup analysis.

In laboratory verification, data was presented as the mean \pm SEM at least three duplications of different samples. Student's *t*-test was applied for analysis between two groups and one-way analysis of variance (ANOVA) was used for comparisons between multiple groups. Statistical analysis was performed with Stata 16.0 software. GraphPad Prism 7.0 (GraphPad Software Inc., United States) were used to analyze and illustrate the data. Differences with *p*-values < 0.05 were considered statistically significant.

Results

Clinical data analysis

Fifteen patients with severe sepsis or septic shock meeting entry criteria were enrolled into the trial. A control group of fifteen individuals was established at a 1:1 ratio. Baseline characteristics of enrolled patients were listed in **Table 1**. In addition to the common indicators (white cell count, C-reactive protein, etc.) for indications that differed significantly between the two groups, the level of LCN-2 in plasma was also markedly higher in SS (median: 87.8 [64.5, 209.2] ng/ml, mean: 158.32 \pm 140.61 ng/ml) than in control group (median: 43.2 [32.6, 94.3] ng/ml, mean: 60.19 \pm 38.67 ng/ml) with statistical difference (*P* = 0.015). Scatter plots of plasma LCN-2 levels showed it fluctuated greatly in patients with severe sepsis (**Figure 1A**), requiring further subgroup analysis. The ROC

revealed LCN-2 was a predictor for sepsis (cut-off value = 75.57 ng/ml, AUC = 0.8067, *P* = 0.0042) (**Figure 1B**).

In the subgroup analysis of sepsis group, the sample was categorized according to the 75th percentile of LCN-2 (179 μ g/l) as mentioned above into Low LCN-2 group (LCN-2 < 179 μ g/l) and High LCN-2 group (LCN-2 \geq 179 μ g/l). Vital signs indicators, along with important cardiac-related biomarkers were compared and analyzed between two subgroups in **Table 2**. The High LCN-2 group had a higher APACHE II score (*P* = 0.006) on admission. All patients required inotropic or vasopressor support in both subgroups. Patients with high level of LCN-2 have a higher level of pro-B-type natriuretic peptide (pro-BNP) (6490 vs. 2510 pg/ml, *P* = 0.005), cardiac troponin I (cTNI) (0.135 vs. 0.02 ng/l, *P* = 0.067), myoglobin (MYO) (487.7 \pm 156.9 ng/l, *P* = 0.055) and CK-MB (12.60 vs. 2.05 ng/l, *P* = 0.009) than those with low level of LCN-2.

A lower ejection fraction (EF) was more common in the High LCN-2 group than in the Low LCN-2 group (*P* = 0.019). Arrhythmia was more frequently observed in High LCN-2 group (75.0%) than in Low LCN-2 group (18.2%) (*P* = 0.039), among which new-onset atrial fibrillation was most common.

Differentially expressed genes identification and analysis based on gene expression omnibus database

GSE28750 and GSE57065 were used for screening differentially expressed genes (DEGs) for bioinformatic analysis. GSE28750 was consisted of 38 sepsis samples and 20 control samples, and GSE57065 covered 28 sepsis samples and control samples. The DEGs were initially prescreened according to the strict criteria of *P*-value < 0.01 and |log FC| > 2. Finally, 99 upregulated and 65 downregulated common DEGs were recognized for further analysis (**Figures 2A,B**). In addition, the common DEGs were presented in **Supplementary Table 2**.

All 164 DEGs consisted of 99 upregulated DEGs and 65 downregulated DEGs were analyzed *via* online tools, the results of which were presented in **Figure 2**. As is shown in **Supplementary Tables 3, 4**, for biological processes (BP), upregulated DEGs were enriched in myeloid leukocyte activation, neutrophil degranulation, neutrophil activation involved in immune response, neutrophil-mediated immunity and neutrophil activation. For cellular components (CC), upregulated DEGs were enriched in secretory granule, specific granule, secretory vesicle, tertiary granule and cytoplasmic vesicle part. For molecular functions, upregulated DEGs were particularly gathered in protein homodimerization activity, carbohydrate kinase activity, 6-phosphofructo-2-kinase activity, catalytic activity and fructose-2,6-bisphosphate 2-phosphatase activity (**Supplementary Figure 1**).

Moreover, DEGs related pathways were enriched by GO (**Figure 2C**) and KEGG (**Figure 2D**) pathway enrichment.

TABLE 2 Cardiac-related characteristics in Low/High LCN-2 subgroup.

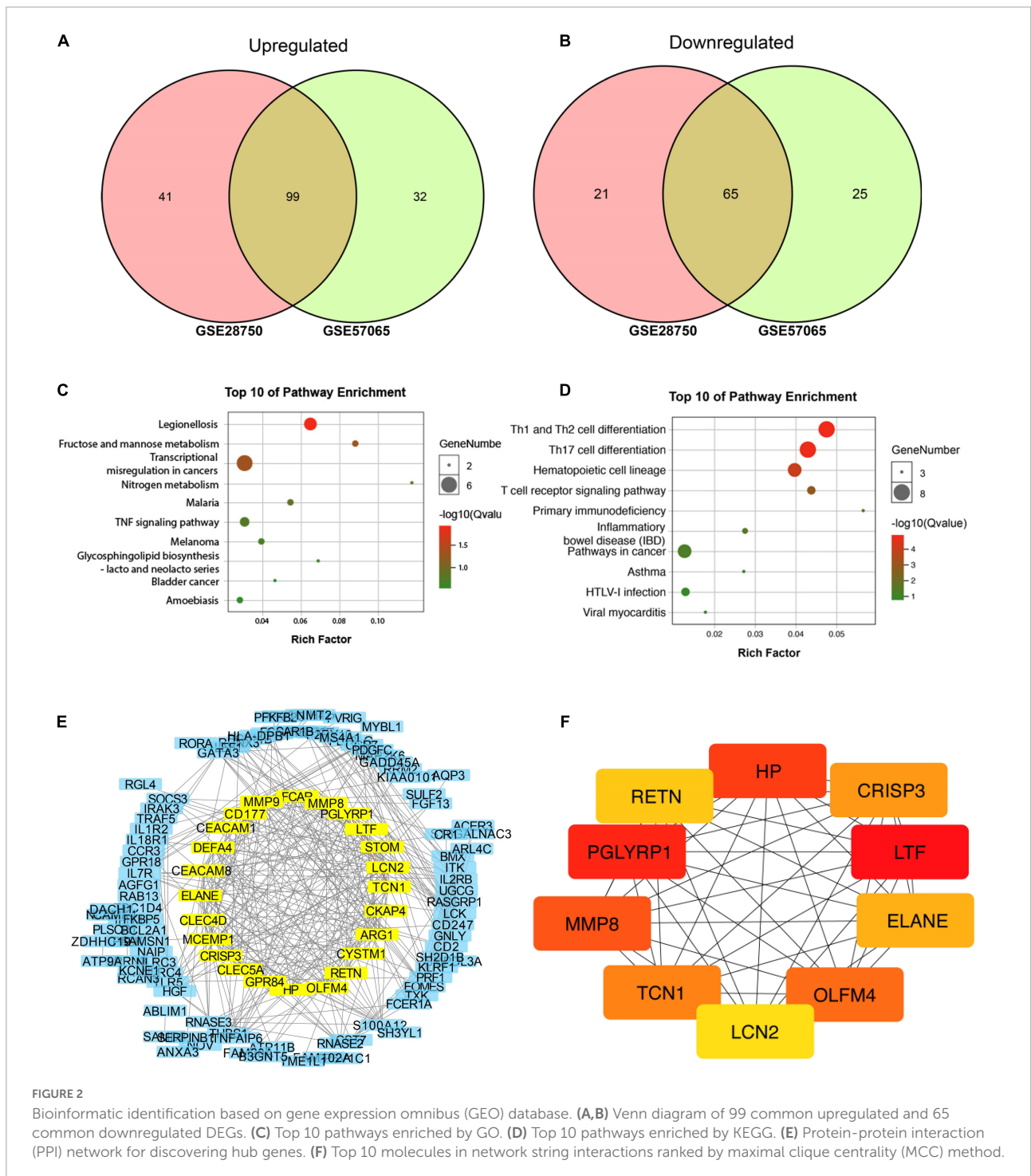
Variable	Low LCN-2 (<179)	High LCN-2 (\geq 179)	<i>P</i> -value
APACHE-II score	25.1 \pm 5.7	36.0 \pm 5.9	0.006
Length of stay in ICU	17.0 \pm 8.0	30.8 \pm 17.0	0.048
Death (%)	3 (27.3)	2 (50)	0.409
Inotropic/vasopressor support (%)	11 (100)	4 (100)	> 0.999
CVP (mmHg)	4.1 \pm 2.2	9.7 \pm 3.9	0.003
MAP (mmHg)	57.9 \pm 10.3	43.8 \pm 9.5	0.033
Pro-BNP (pg/ml)	2510 [1420, 3390]	6490 [4290, 9790]	0.005
cTNI (ng/l)	0.02 [0.01, 0.04]	0.135 [0.09, 1.51]	0.067
MYO (ng/l)	156.9 [33.2, 339.4]	487.7 [212.7, 2219.4]	0.055
CK-MB (ng/l)	2.05 [0.80, 5.09]	12.60 [10.05, 24.11]	0.009
Arrhythmia (%)	2 (18.2)	3 (75.0)	0.039
Ejection fraction (%)	64 [62, 65]	56 [52, 59]	0.019

CK-MB, creatine kinase MB isoenzyme; cTNI, cardiac troponin I; CVP, central venous pressure; MAP, mean venous pressure; MYO, myoglobin.

Then STRING database was applied to build a PPI network for discovering hub genes (Figure 2E). Ten hub genes were obtained in network string interactions ranked by maximal clique centrality (MCC) method (Figure 2F), among which LCN-2 showed preferable significance, along with several molecules reported to be related to lipid or other metabolism including PGRPs, OLFM4, RETN etc.

Validation on animal models

The mouse model of SIC group ($n = 6$) and control groups ($n = 6$) were successfully established. Together with LCN-2, three secreted molecules chosen from the results of the bioinformatic analysis were assayed from the plasma at 12 h after LPS stimulation (Figures 3A-C). The level of LCN-2 was



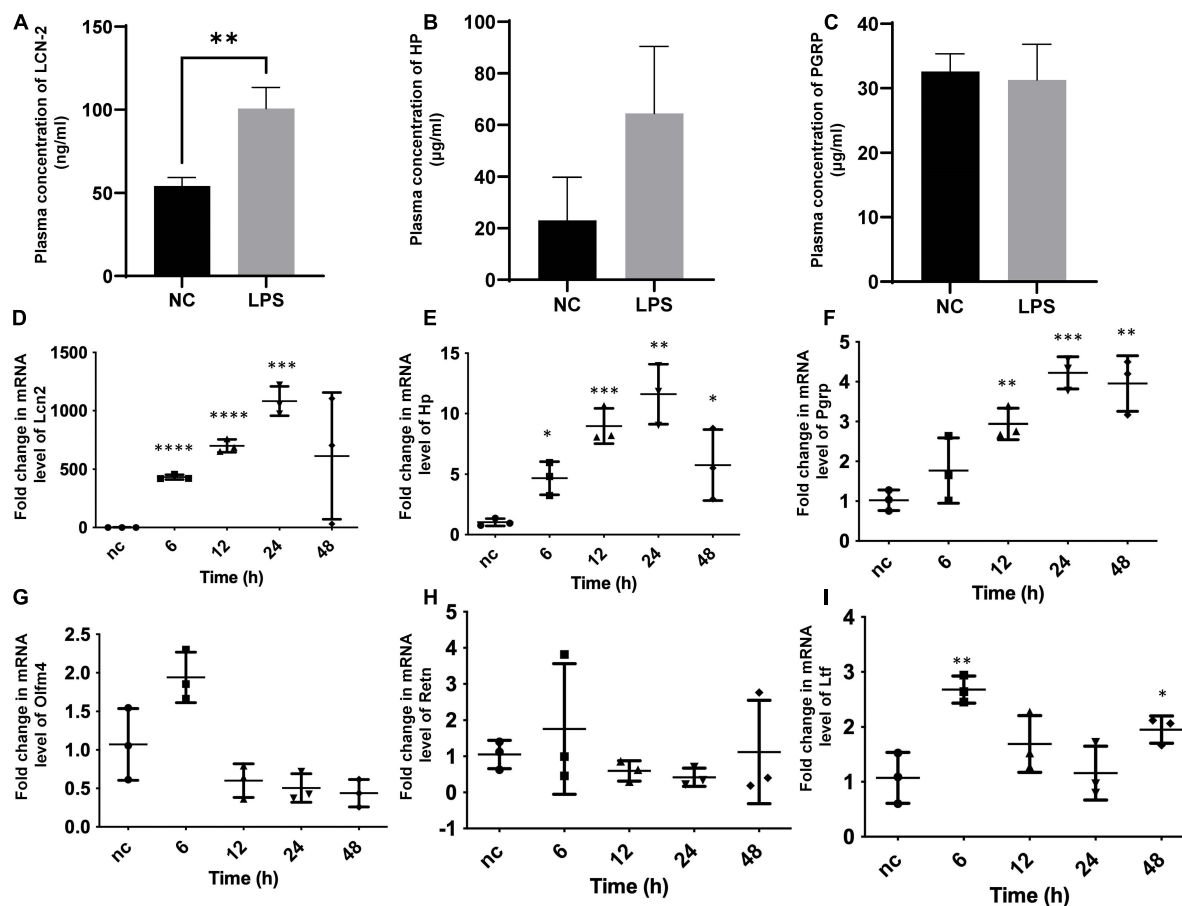


FIGURE 3

Plasma assay for circulating concentration and qPCR of myocardial tissue for cardiac mRNA determination in *SIC* mouse. (A–C) Plasma concentration of LCN-2, HP, PGRP of both groups at 12 h after the induction of LPS. (D–I) Fold change in mRNA level of Lcn2, Hp, Pgrp, Olfm4, Retn, Ltf of myocardial tissue at different times testing by qPCR. Hp, haptoglobin; Lcn2, lipocalin-2; Ltf, lactotransferrin; Olfm4, olfactomedin-4; Pgrp, peptidoglycan recognition protein-1; Retn, resistin. * $P < 0.05$, ** $P < 0.01$, *** $P < 0.001$, and **** $P < 0.0001$.

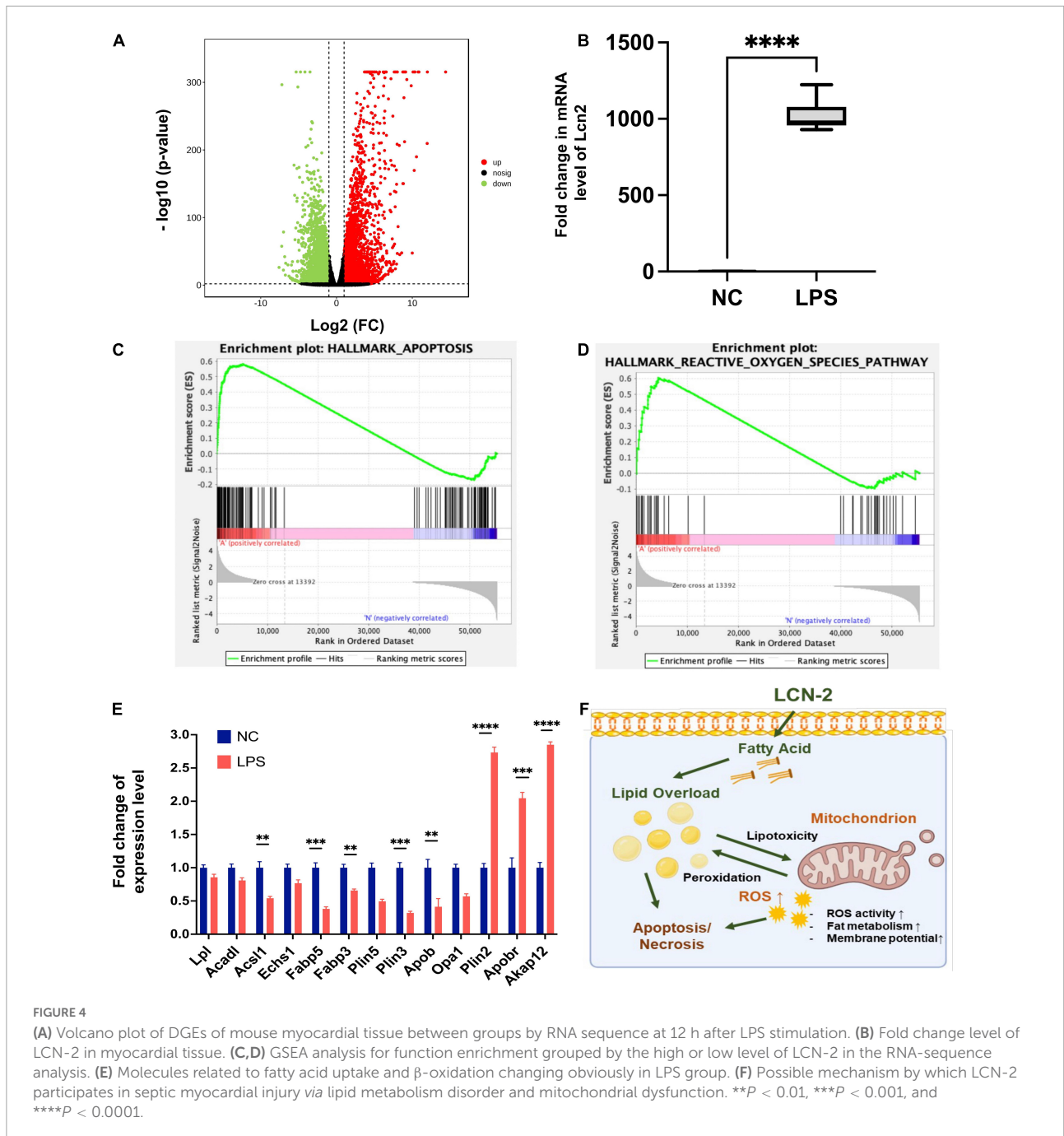
significantly higher (100.7 ± 31.0 ng/ml) in *SIC* group than in control group (54.2 ± 12.6 ng/ml) ($P = 0.007$).

For further identification and exploration, the mRNA of myocardial tissue was extracted at different times (0, 6, 12, 24, 48 h) from the onset of *SIC* (Figures 3D–I), LCN-2 and other molecules chosen from the results of the bioinformatic analysis were assayed for each stage. LCN-2 demonstrated a high level of transcription in the heart tissue and showed a clear time relationship with significant change at the 6th hour and peak at the 24th hour.

RNA sequencing and analysis

RNA sequencing analysis of myocardial tissue from 12 mice (LPS, $n = 6$; NC, $n = 6$) was shown in Figures 4A,B and Supplementary Figure 2, DEGs consisted of 2127 upregulated DEGs and 1687 downregulated DEGs were detected (Figure 4A). Pathways enrichment by GO and KEGG were

shown in Supplementary Figure 2. Fold change level of LCN-2 in myocardial tissue in LPS group was almost 1,000 times than NC group ($P < 0.001$) (Figure 4B). GSEA analysis for function enrichment grouped by the high or low level of LCN-2 (using the cut-off value calculated by Receiver Operator Characteristic curve, FPKM: 913.8) showed the level of LCN-2 was strongly associated with cell apoptosis, ROS, adipogenesis and cholesterol homeostasis (top 20 pathway enriched) (Figures 4C,D and Supplementary Figures 3A,B). In addition, many fatty acid metabolism-related molecules, including LPL, ACSL1, FABPs, PLINs, etc., which were relevant with mitochondrial function and previously reported to be mediated by LCN-2, changed obviously in LPS group (Figure 4E and Supplementary Figure 3C). The level of STAT3 also significantly increased, which was reported to be the transcription factor of LCN-2 (Supplementary Figure 3D). Thus, we speculated LCN-2 could probably participate in *SIC* and be associated with myocardial injury.



Functional verification for mitochondria damage and lipid accumulation

The mitochondrial morphology and ROS level were assayed by MitoTracker™ and DCFH-DA assessment at 12 h after LPS stimulation, which showed disordered mitochondria with abnormal appearance and increased ROS level after LPS induction. By contrast, when cardiomyocytes were pretreated

with LCN2-siRNA (siLCN2), the normal mitochondrial structure was restored to some extent and ROS level was decreased (Figure 5).

Estimation of the mitochondrial membrane potential using the JC-1 probe demonstrated that the LPS stimulation obviously decreased the mitochondrial membrane potential (decreased JC-1 aggregates, red; increased JC-1 monomer, green), suggesting mitochondrial function damage. In contrast, treatment by siLCN2 significantly increased the level of mitochondrial membrane potential (JC-1 aggregates, red),

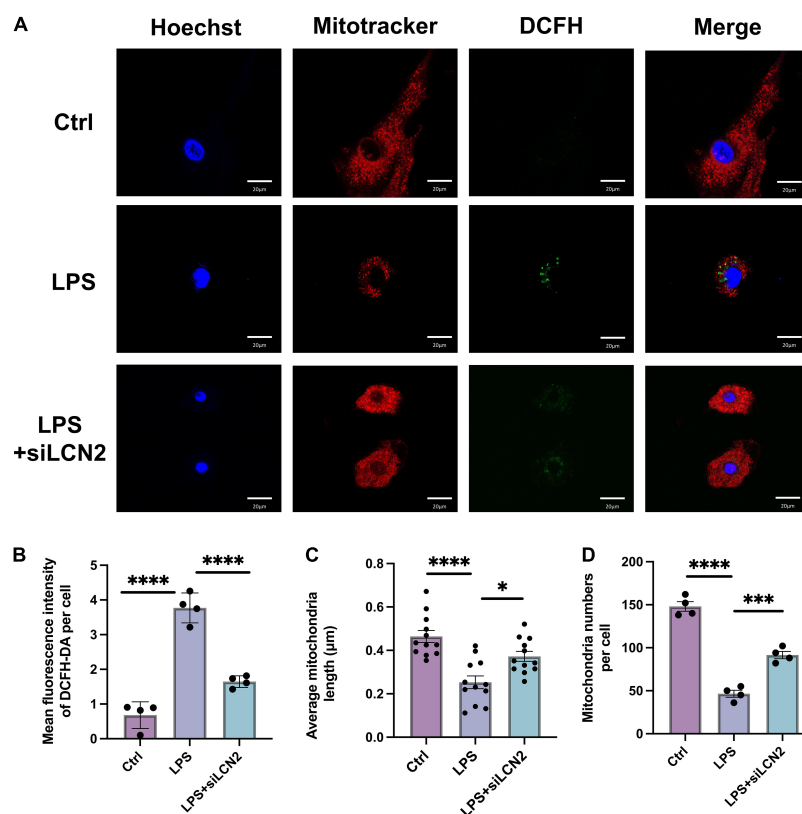


FIGURE 5

The suppression of LCN-2 protected mitochondrial morphology and limited the production of ROS. (A) Mitochondrial morphology (MitoTracker, red) and ROS level (DCFH-DA, green) of LPS damaged H9C2 cardiomyocytes pretreated with siLCN2 ($n = 3$; scale bar = 20 μm). (B) Mean fluorescence intensity of DCFH-DA ($n = 4$). (C) Average mitochondria length of cardiomyocytes in TEM ($n = 12$). (D) Average number of mitochondria of cardiomyocytes ($n = 4$). Data are presented as mean \pm SEM. Statistical analysis was via one-way ANOVA with Bonferroni multiple-comparison correction; * $P < 0.05$, ** $P < 0.01$, *** $P < 0.001$, and **** $P < 0.0001$.

indicating restored mitochondrial function after siLCN2 treatment (Figure 6).

Lipid metabolism is indispensable for maintaining normal mitochondria function. Neutral lipid staining was then performed at 12 h after the stimulation of LPS using HCS LipidTOXTM and showed prominent lipid accumulation in LPS group, which was alleviated by the treatment of siLCN2 (Figure 7 and Supplementary Figure 4 for quantification), indicating LCN-2 may participate in the process of septic myocardial injury via inducing lipid accumulation and mitochondrial dysfunction (Figure 4F). Further explorations for detailed mechanisms could be conducted in the following studies.

Discussion

Sepsis-induced cardiomyopathy is one of the leading causes of death for sepsis (3). However, it often lacks timely diagnosis and specific treatment due to the uncertain mechanism and

diagnostic criteria (4). Thus, it is helpful to find valuable biomarkers assisting the diagnosis and treatment of SIC.

LCN-2 has been recognized as a promising inflammatory marker involved in many acute inflammatory damages in many diseases such as acute kidney injury, ischemic stroke, myocardial ischemia-reperfusion injury, etc. (16, 18, 27, 28). It participates in various pathological processes via multiple immune or inflammation-related mechanisms in diverse situations, leading to the inconsistent results based on different cell types and conditions (29–31). In this study, we focus on the acute-phase of sepsis-induced myocardial injury where the role of LCN-2 remains unclear, and found a strong relationship with myocardial damage based on clinical and laboratory evidence.

In current study, the level of LCN-2 was much higher in plasma in severe sepsis patients which is similar to previous reports (19, 32). In the subgroup analysis, amongst the population with sepsis, patients with a higher level of LCN-2 demonstrated higher cardiac markers and lower LVEF, etc., indicating LCN-2 was potentially associated with septic myocardial injury.

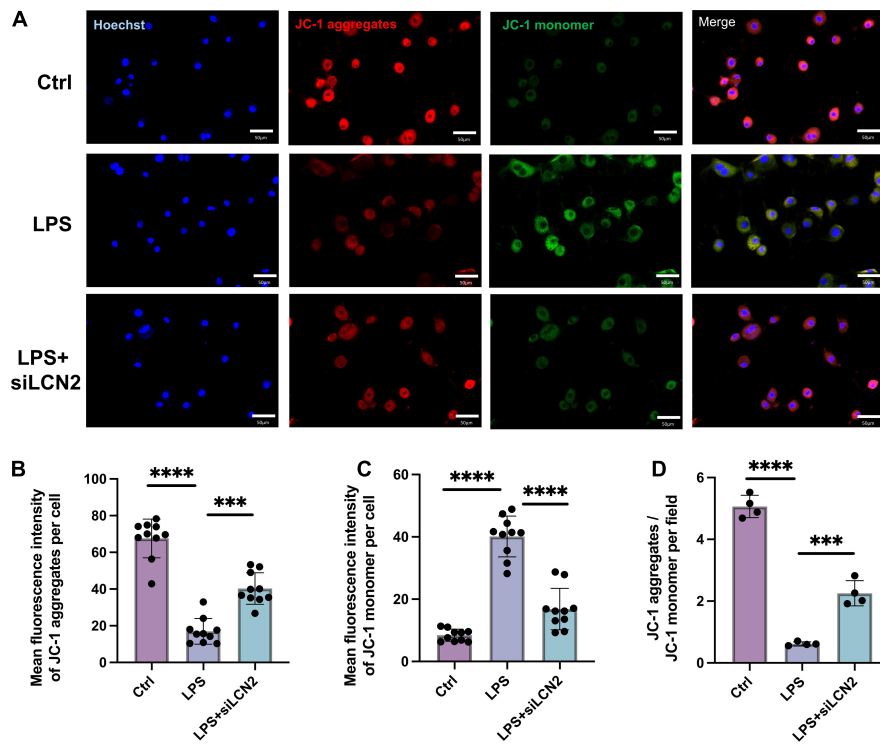


FIGURE 6

Silence of LCN-2 restored the mitochondrial membrane potential damaged by LPS. (A) Mitochondrial membrane potential (JC-1) of LPS damaged H9C2 cardiomyocytes pretreated with siLCN2. Red indicated JC-1 aggregates and green indicated JC-1 monomer ($n = 3$, scale bar = 50 μm). (B–D) Quantitative results of mitochondrial membrane potential. Data are presented as mean \pm SEM. Statistical analysis was via one-way ANOVA with Bonferroni multiple-comparison correction, ** $P < 0.01$, *** $P < 0.001$, and **** $P < 0.0001$.

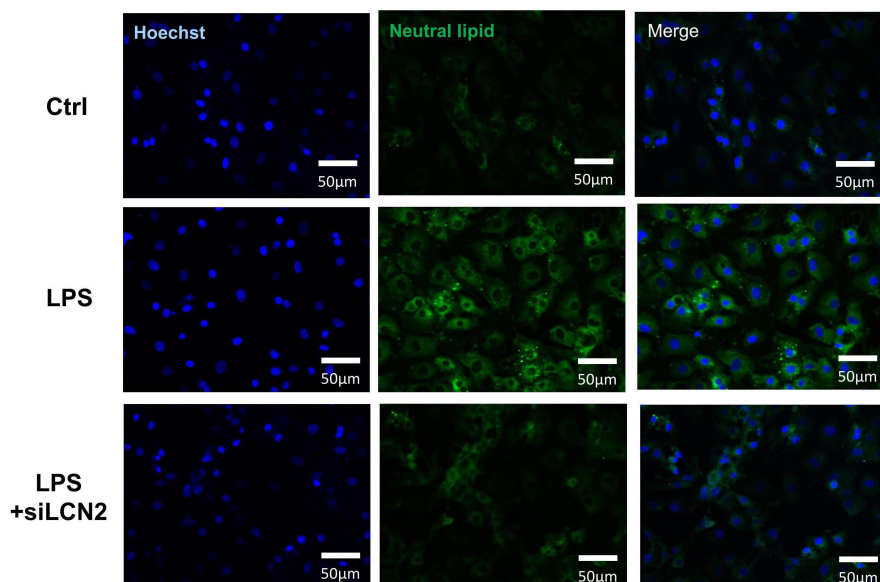


FIGURE 7

Neutral lipid staining of LPS damaged H9C2 cardiomyocytes at 12h after LPS stimulation. The inhibition of LCN-2 alleviated the lipid accumulation in H9C2 cells caused by LPS stimulation.

Microarray analysis in transcriptome profile has been used as a valuable laboratory tool to identify critical genes and signaling pathways involved in pathogenesis and solve the limitation of clinical sample size (33). Transcriptome profiling usually yields a considerable number of potential differential transcripts, which is a challenge to identify the critical genes. A pooled biostatistical analysis of a transcriptome array dataset which combines multiple species may help screen conservative and important genes involved in a given disorder (34). In the bioinformatic analysis, LCN-2 showed great significance, along with several modules reported to be related to lipid or other metabolism.

In vivo, circulating LCN-2 from plasma was verified to increase in SIC mice. In order to seek a more direct connection with myocardial tissue, the level of LCN-2 from septic myocardial tissue was tested, which as a result, demonstrated a high level of transcription in the heart tissue, and showed a clear time dependence with significant change at the 6th hour and peak at 24th hour, providing more direct evidence of the relationship between LCN-2 and LPS-induced myocardial injury.

Mitochondrial dysfunction is a well-recognized mechanism in SIC (3, 4). In the RNA-sequence analysis, the level of LCN-2 was strongly associated with cell apoptosis, ROS, using GSEA for function enrichment grouped by the high or low level of *Lcn2*. Moreover, the suppression of LCN-2 protected mitochondrial morphology and limited the production of ROS, as well as restored the mitochondrial membrane potential damaged by LPS, indicating LCN-2 may participate the process of mitochondrial dysfunction.

Lipid metabolism is indispensable for maintaining normal mitochondria function (5, 35), while lipotoxicity, often caused by lipid overload, has been reported in multiple cardiac pathological processes by influencing mitochondrial function (36–38). LCN-2 is reported to be responsible for the transportation of small lipophilic molecules such as lipids (13, 14). Through analyzing the change of differential genes in LPS-induced cardiac injury by RNA sequencing, LCN-2 and other relevant molecules related to fatty acid uptake and β -oxidation changed obviously which participated in mitochondrial activity. In addition, neutral lipid staining showed prominent lipid accumulation in LPS group, which was alleviated by the suppression of LCN-2, indicating LCN-2 may participate in the process of septic myocardial injury *via* inducing lipid accumulation and mitochondrial dysfunction. Further explorations for detailed mechanisms could be conducted in the following studies.

Conclusion

The level of LCN-2 is significantly increased in SIC at both circulating and tissue level, which is correlated with the

severity of myocardial injury indicators, and may work as an early and great predictor of SIC in clinical practice. LCN-2 probably participates in the process of septic myocardial injury through mediating lipid accumulation and affecting mitochondrial function.

Data availability statement

The datasets presented in this study can be found in online repositories. The names of the repository/repositories and accession number(s) can be found in the article/**Supplementary material**.

Ethics statement

The studies involving human participants were reviewed and approved by Institutional Review Board (IRB) for Human Research at Shanghai Chest Hospital, Shanghai Jiao Tong University. The patients/participants provided their written informed consent to participate in this study. The animal study was reviewed and approved by Animal Ethics Committee of Shanghai Chest Hospital.

Author contributions

WL, XG, SL, and BH designed the study. LJ was responsible for the collection of clinical samples. BH supervised the whole work. WL and XG drafted the manuscript. All authors contributed to the data collection or analysis, reviewed it for important scientific content, and approved the final version of this manuscript.

Funding

This work was supported by the National Natural Science Foundation of China (No. 82072199), the Clinical Research Plan of Shanghai Hospital Development Center (No. SHDC2020CR3084B), Interdisciplinary Program of Shanghai Jiao Tong University (Nos. YG2022QN101 and YG2022ZD025), and the Shanghai Collaborative Innovation Center for Translational Medicine Fund (NO.TM202013).

Acknowledgments

We thank the medical and paramedical staff of their intensive care units, for the help for supporting clinical research provided during these hard times.

Conflict of interest

The authors declare that the research was conducted in the absence of any commercial or financial relationships that could be construed as a potential conflict of interest.

Publisher's note

All claims expressed in this article are solely those of the authors and do not necessarily represent those of their affiliated

organizations, or those of the publisher, the editors and the reviewers. Any product that may be evaluated in this article, or claim that may be made by its manufacturer, is not guaranteed or endorsed by the publisher.

Supplementary material

The Supplementary Material for this article can be found online at: <https://www.frontiersin.org/articles/10.3389/fcvm.2022.1009726/full#supplementary-material>

References

- Evans L, Rhodes A, Alhazzani W, Antonelli M, Coopersmith CM, French CE, et al. Surviving sepsis campaign: international guidelines for management of sepsis and septic shock 2021. *Intensive Care Med.* (2021). 47:1181–247.
- Prescott HC, Angus DC. Enhancing recovery from sepsis: a review. *JAMA.* (2018) 319:62–75. doi: 10.1001/jama.2017.17687
- Hollenberg SM, Singer M. Pathophysiology of sepsis-induced cardiomyopathy. *Nat Rev Cardiol.* (2021) 18:424–34. doi: 10.1038/s41569-020-00492-2
- L'Heureux M, Sternberg M, Brath L, Turlington J, Kashiouris MG. Sepsis-induced cardiomyopathy: a comprehensive review. *Curr Cardiol Rep.* (2020) 22:35. doi: 10.1007/s11886-020-01277-2
- Benador IY, Veliova M, Liesa M, Shirihai OS. Mitochondria bound to lipid droplets: where mitochondrial dynamics regulate lipid storage and utilization. *Cell Metab.* (2019) 29:827–35. doi: 10.1016/j.cmet.2019.02.011
- Stanzani G, Duchon MR, Singer M. The role of mitochondria in sepsis-induced cardiomyopathy. *Biochim Biophys Acta Mol Basis Dis.* (2019) 1865:759–73. doi: 10.1016/j.bbadis.2018.10.011
- Ducasa GM, Mitrofanova A, Fornoni A. Crosstalk between lipids and mitochondria in diabetic kidney disease. *Curr Diab Rep.* (2019) 19:144. doi: 10.1007/s11892-019-1263-x
- Nakamura H, Matoba S, Iwai-Kanai E, Kimata M, Hoshino A, Nakaoka M, et al. p53 promotes cardiac dysfunction in diabetic mellitus caused by excessive mitochondrial reactive oxygen species in lipotoxic hearts induce post-translational modifications of AKAP121, DRP1, and OPA1 that promote mitochondrial fission. *Circ Heart Fail.* (2012) 5:106–15. doi: 10.1161/CIRCHEARTFAILURE.111.961565
- Tsushima K, Bugger H, Wende AR, Soto J, Jenson GA, Tor AR, et al. Mitochondrial reactive oxygen species in lipotoxic hearts induce post-translational modifications of AKAP121, DRP1, and OPA1 that promote mitochondrial fission. *Circ Res.* (2018) 122:58–73. doi: 10.1161/CIRCRESAHA.117.311307
- Amunugama K, Pike DP, Ford DA. The lipid biology of sepsis. *J Lipid Res.* (2021) 62:100090. doi: 10.1016/j.jlr.2021.100090
- Chung KW, Kim KM, Choi YJ, An HJ, Lee B, Kim DH, et al. The critical role played by endotoxin-induced liver autophagy in the maintenance of lipid metabolism during sepsis. *Autophagy.* (2017) 13:1113–29. doi: 10.1080/15548627.2017.1319040
- Guo X, Hong T, Zhang S, Wei Y, Jin H, Miao Q, et al. IL-13 alleviates cardiomyocyte apoptosis by improving fatty acid oxidation in mitochondria. *Front Cell Dev Biol.* (2021) 9:736603. doi: 10.3389/fcell.2021.736603
- Jaberi SA, Cohen A, D'Souza C, Abdulrazzaq YM, Ojha S, Bastaki S, et al. Lipocalin-2: structure, function, distribution and role in metabolic disorders. *Biomed Pharmacother.* (2021) 142:112002. doi: 10.1016/j.biopha.2021.112002
- Li D, Yan Sun W, Fu B, Xu A, Wang Y. Lipocalin-2—the myth of its expression and function. *Basic Clin Pharmacol Toxicol.* (2020) 127:142–51. doi: 10.1111/bcpt.13332
- Xiao X, Yeoh BS, Vijay-Kumar M. Lipocalin 2: an emerging player in iron homeostasis and inflammation. *Annu Rev Nutr.* (2017) 37:103–30. doi: 10.1146/annurev-nutr-071816-064559
- Marques FZ, Prestes PR, Byars SG, Ritchie SC, Würtz P, Patel SK, et al. Experimental and human evidence for lipocalin-2 (neutrophil gelatinase-associated lipocalin [NGAL]) in the development of cardiac hypertrophy and heart failure. *J Am Heart Assoc.* (2017) 6:e005971. doi: 10.1161/JAHA.117.005971
- Jang HM, Lee JY, An HS, Ahn YJ, Jeong EA, Shin HJ, et al. LCN2 deficiency ameliorates doxorubicin-induced cardiomyopathy in mice. *Biochem Biophys Res Commun.* (2022) 588:8–14. doi: 10.1016/j.bbrc.2021.12.048
- Sung HK, Chan YK, Han M, Jahng JWS, Song E, Danielson E, et al. Lipocalin-2 (NGAL) attenuates autophagy to exacerbate cardiac apoptosis induced by myocardial ischemia. *J Cell Physiol.* (2017) 232:2125–34. doi: 10.1002/jcp.25672
- Lu F, Inoue K, Kato J, Morisaki H. Functions and regulation of lipocalin-2 in gut-origin sepsis: a narrative review. *Crit Care.* (2019) 23:269. doi: 10.1186/s13054-019-2550-2
- Mertens C, Kuchler L, Sola A, Guiteras R, Grein S, Brüne B, et al. Macrophage-derived iron-bound lipocalin-2 correlates with renal recovery markers following sepsis-induced kidney damage. *Int J Mol Sci.* (2020) 21:7527. doi: 10.3390/ijms21207527
- Barrett T, Wilhite SE, Ledoux P, Evangelista C, Kim IF, Tomashevsky M, et al. NCBI GEO: archive for functional genomics data sets—update. *Nucleic Acids Res.* (2012) 41:D991–5. doi: 10.1093/nar/gks1193
- Ashburner M, Ball CA, Blake JA, Botstein D, Butler H, Cherry JM, et al. Gene ontology: tool for the unification of biology. *Nat Genet.* (2000) 25:25–9. doi: 10.1038/75556
- Kanehisa M, Goto S. KEGG: kyoto encyclopedia of genes and genomes. *Nucleic Acids Res.* (2000) 28:27–30. doi: 10.1093/nar/28.1.27
- Hong T, Li S, Guo X, Wei Y, Zhang J, Su X, et al. IL-13 derived type 2 innate lymphocytes ameliorates cardiomyocyte apoptosis through STAT3 signaling pathway. *Front Cell Dev Biol.* (2021) 9:742662. doi: 10.3389/fcell.2021.742662
- Son DH, Ha HS, Lee YJ. Association of serum alkaline phosphatase with the TG/HDL ratio and TyG index in Korean adults. *Biomolecules.* (2021) 11:882. doi: 10.3390/biom11060882
- Dores H, Gonçalves PA, Monge J, Costa R, Tátá L, Cardim N, et al. Coronary atherosclerotic burden in veteran male recreational athletes with low to intermediate cardiovascular risk. *Rev Port Cardiol.* (2020) 39:587–94. doi: 10.1016/j.repc.2019.10.009
- Shang W, Wang Z. The update of NGAL in acute kidney injury. *Curr Protein Pept Sci.* (2017) 18:1211–7. doi: 10.2174/1389203717666160909125004
- Suk K. Lipocalin-2 as a therapeutic target for brain injury: an astrocentric perspective. *Prog Neurobiol.* (2016) 144:158–72. doi: 10.1016/j.pneurobio.2016.08.001
- Sickinger S, Maier H, König S, Vallant N, Kofler M, Schumpp P, et al. Lipocalin-2 as mediator of chemokine expression and granulocyte infiltration during ischemia and reperfusion. *Transpl Int.* (2013) 26:761–9. doi: 10.1111/tri.12116
- Cheng L, Xing H, Mao X, Li L, Li X, Li Q. Lipocalin-2 promotes m1 macrophages polarization in a mouse cardiac ischaemia-reperfusion injury model. *Scand J Immunol.* (2015) 81:31–8. doi: 10.1111/sji.12245

31. Ferreira AC, Dá Mesquita S, Sousa JC, Correia-Neves M, Sousa N, Palha JA, et al. From the periphery to the brain: lipocalin-2, a friend or foe? *Prog Neurobiol.* (2015) 131:120–36. doi: 10.1016/j.pneurobio.2015.06.005
32. Vazquez DE, Niño DF, De Maio A, Cauvi DM. Sustained expression of lipocalin-2 during polymicrobial sepsis. *Innate Immun.* (2015) 21:477–89. doi: 10.1177/1753425914548491
33. Segundo-Val IS, Sanz-Lozano CS. Introduction to the gene expression analysis. *Methods Mol Biol.* (2016) 1434:29–43. doi: 10.1007/978-1-4939-3652-6_3
34. Head SR, Mondala T, Gelbart T, Ordoukhanian P, Chappel R, Hernandez G, et al. RNA purification and expression analysis using microarrays and RNA deep sequencing. *Methods Mol Biol.* (2013) 1034:385–403. doi: 10.1007/978-1-62703-493-7_25
35. Schrauwen P, Schrauwen-Hinderling V, Hoeks J, Hesselink MK. Mitochondrial dysfunction and lipotoxicity. *Biochim Biophys Acta.* (2010) 1801:266–71. doi: 10.1016/j.bbaliip.2009.09.011
36. D'Souza K, Nzirorera C, Kienesberger PC. Lipid metabolism and signaling in cardiac lipotoxicity. *Biochim Biophys Acta.* (2016) 1861:1513–24. doi: 10.1016/j.bbaliip.2016.02.016
37. Li H, Fan J, Zhao Y, Zhang X, Dai B, Zhan J, et al. Nuclear miR-320 mediates diabetes-induced cardiac dysfunction by activating transcription of fatty acid metabolic genes to cause lipotoxicity in the heart. *Circ Res.* (2019) 125:1106–20. doi: 10.1161/CIRCRESAHA.119.314898
38. Tong M, Saito T, Zhai P, Oka SI, Mizushima W, Nakamura M, et al. Mitophagy is essential for maintaining cardiac function during high fat diet-induced diabetic cardiomyopathy. *Circ Res.* (2019) 124:1360–71. doi: 10.1161/CIRCRESAHA.118.314607